https://doi.org/10.5194/egusphere-2026-6628
Preprint. Discussion started: 30 October 2026
© Author(s) 2026. CC BY 4.0 License.

Projecting multi-scale sub-daily extreme rainfall distributions from Convection-Permitting Climate simulations: Implications for Intensity–Duration–Frequency curves in the West African Sahel

Laura Marimbordes[1], Theo Vischel[1], Geremy Panthou[1], Thierry Lebel[1], Guillaume Chagnaud[2], and Youssouph Sane[3]

[1]Univ. Grenoble Alpes, CNRS, INRAE, IRD, Grenoble INP, IGE, Grenoble, France
[2]UK Centre for Ecology and Hydrology, Wallingford, UK
[3]Agence Nationale de l'Aviation Civile et de la Météorologie (ANACIM), Dakar, Senegal

Correspondence: Laura Marimbordes (laura.marimbordes@univ-grenoble-alpes.fr)

Abstract. Reliable characterization of extreme rainfall across a continuum of temporal scales is fundamental to hydrological applications, from flood risk assessment to the design of water infrastructure. In a changing climate, however, characterizing this continuum is particularly challenging, as both the distribution of extreme rainfall and its temporal scaling may evolve. Convection-permitting models (CPMs), which explicitly represent convection and provide precipitation at high spatial and temporal resolutions, offer promising opportunities to address this challenge. Yet, their added value for hydrological applications remains poorly explored, particularly regarding model biases and their ability to consistently represent and project extreme rainfall across timescales. We develop a methodological framework to project extreme rainfall distributions from from CPM simulations. The framework combines the identification of potential CPM biases with indicators of simulated changes in extreme rainfall distributions to guide the selection of analytical and empirical approaches for addressing these biases. Extreme rainfall is characterized across durations spanning 2 to 24 hours using synthetic intensity-duration-frequency (IDF) curves based on extreme value and simple scaling theories. The methodology is illustrated over the West African Sahel using CP4-Africa simulations to project locally observed IDF curves under future climate conditions. Onto the Niamey region, results indicate a substantial decrease in the return periods for given extreme rainfall intensities. The simulations are further analyzed to assess the applicability of the framework and guide projections across the Sahelian region. Its generic nature makes the methodology transferable to other regions, given the growing number of climate modeling initiatives based on CPM simulations worldwide.

1 Introduction

As anticipated in the 2000's, based on theoretical considerations (Allen and Ingram, 2002; Trenberth et al., 2003), and as now largely observed over the past 15 years or so, global warming is profoundly impacting rainfall regimes worldwide (Allan et al., 2020). Both the occurrence and the intensity of rainfall events are modified, leading to an intensification of the hydrological cycle that involves a reinforcement of extreme rainfalls over a large range of time duration (Westra et al., 2013; Dunn et al.,

https://doi.org/10.5194/egusphere-2026-6628
Preprint. Discussion started: 30 October 2026
© Author(s) 2026. CC BY 4.0 License.

2020). This, in turn, is challenging the engineering practices and techniques on which hydrologists rely for dimensioning and managing the infrastructures used for water resources management and flood control(Milly et al., 2008; François et al., 2019; Sharma et al., 2021). The cornerstone of these techniques is to address the multi-dimensional nature of hydrological processes that are not linearly additive when upscaling in space or in time, which is especially true for rainfall generating processes. Because they may have to deal simultaneously with catchments of different sizes, hydrologists have developed scaling approaches that guarantee a coherent representation of rainfall regimes through time and areal scales (Blöschl and Sivapalan, 1995). The inference of the attached statistical parameters requires long series of observations assuming stationarity to be an acceptable hypothesis. As mentioned above this no longer holds in the context of global warming and there is no guarantee that the statistical distributions of rainfall accumulation are affected in similar proportion on all timescales. In such a situation, hydrologists can but rely on climate models and their ability to produce warmer world rainfall climatologies for assessing i) how rainfall statistical distributions are modified for a given time step and ii) whether scaling properties over a range of time scales are conserved or not.

While it is generally accepted that global and regional climate models (GCMs/RCMs) with a resolution higher than 10 km reproduce daily extreme rainfall satisfactorily, their ability to simulate sub-daily extremes remains limited (Martel et al., 2021). In particular, these models tend to underestimate the intensity of extreme rainfall on timescales shorter than a day (Berg et al., 2019). This is especially problematic since the response of extreme rainfall to global warming depends heavily on the temporal scale considered: while daily extreme rainfall generally increases at a rate close to the Clausius–Clapeyron scaling law ($\sim$7%/°C) (Guerreiro et al., 2018; Westra et al., 2013), hourly extreme rainfall often exhibits higher rates of increase, described as "super-Clausius-Clapeyron" (Berg et al., 2013; Lenderink and Van Meijgaard, 2010; Panthou et al., 2014a; Westra et al., 2014). This dependence of rainfall sensitivity on timescales highlights the difficulty of accurately representing the continuum of extreme rainfall—from hourly to daily timescales—in GCMs and RCMS. These models, which are limited by coarse spatial resolution and an approximate parameterization of key processes such as convection and microphysics (Berg et al., 2018; Dosio et al., 2021; Willems, 2012; Kendon et al., 2012), do not meet the needs of hydrologists, who require an accurate representation of extreme rainfall on sub-daily to sub-hourly scales.

Convection-permitting models (CPMs), with a horizontal grid spacing of $\mathcal{O}$(1–10 km), partially overcome this limitation through an explicit representation of deep convection (Kendon et al., 2012; Ban et al., 2014, 2020), leading to a more realistic simulation of extreme rainfall intensities on sub-daily and sub-hourly timescales (Ban et al., 2015; Kendon et al., 2014; Prein et al., 2015). Due to this higher spatial resolution and because they are designed to explicitly simulate the physics of storms these models allow for better consideration of the spatial and temporal scale continuum of precipitation extremes necessary for the development of reliable hydrological impact studies under future climates (Fosser et al., 2024; Martel et al., 2021). However, it remains to be determined whether CPMs are able to accurately reproduce the temporal continuum of extreme rainfall required for hydrological applications—that is, a consistent representation of rainfall over different durations scales relevant to hydrologists and what implications this has for projections of future rainfall extremes.

One of the most commonly used frameworks for documenting the scale continuum is the one provided by the intensity–duration–frequency (IDF) curves (Koutsoyiannis et al., 1998). It is based on a coherent multi-scale statistical characteriza-

https://doi.org/10.5194/egusphere-2026-6628
Preprint. Discussion started: 30 October 2026
© Author(s) 2026. CC BY 4.0 License.

tion of extreme rainfall distribution and is widely used by engineers involved in operational hydrology, whether flood mapping or the design of storm water management infrastructures such as sewers or bridges. Assuming temporal scale invariance (Gupta and Waymire, 1990; Menabde et al., 1999), IDF curves can be determined using only a few parameters (Blanchet et al., 2016; Burlando and Rosso, 1996; Van De Vyver, 2015, 2018). While return period values are typically calculated for different rainfall durations, the IDF-Simple Scaling (IDF-SS) method combines information from all durations into a parsimony-based statistical model by adding an additional scale parameter (η). This method provides a better fit and greater consistency—that is, the absence of overlap in recurrence levels across durations—and allows for the extension of rainfall durations to values within the range of durations used for the fit (Van De Vyver et al., 2023). In a stationary climate, IDF curves were considered a stable and reliable design tool. In the context of climate change, the hydrology community is seeking ways to project IDF curves into the future (Schlef et al., 2023).

The IDF-SS framework has already been adopted for analysing the potential of CPMs, whether be for assessing the realism of CPMs under present climate (Van De Vyver et al., 2021) or for projecting the distribution of extremes rainfall within a scale continuum (see (Cannon and Innocenti, 2019), for Canada and (Nguyen et al., 2025), for the Midwestern United States, both using WRF simulations). In (Cannon and Innocenti, 2019), bias correction was not applied, as the authors considered present rainfall simulated by the WRF convection-permitting model to be sufficiently realistic. Future IDF curves were therefore projected within the IDF-SS framework directly from simulated future rainfall. In a different way, (Nguyen et al., 2025) projected future IDF curves separately for each rainfall duration using the CDF-t bias-correction method, calibrated with observations and applied to both historical and future simulations. The objective of our study is to provide a generic methodological framework that explains how to account for the scale continuum within the theoretical framework of extreme values in simple scaling (IDF-SS). This "step-by-step" method allows us to clarify the assumptions underlying the IDF projection including the bias-correction process. It draws on precipitation simulations from a CPM model, examining the consistency of certain parameters across simulations in present and future climates, while retaining as much information as possible from observation-based IDF reference curves, in order to project future distributions of extreme precipitation at multiple scales. The added value of the methodological framework we propose lies in first guiding the projection of IDF curves toward an analytical approach, and then proposing empirical approaches where appropriate.

This methodology is applied to the West African Sahel, a region where the population is particularly vulnerable to climate change and related hydrological risks generating an urgent demand from regional services responsible for the development and implementation of adaptation strategies for reliable information on future climate conditions (Miller et al., 2022). The IDF curves are first projected locally onto the Niamey region through combining high-spatial- and temporal-resolution data from the AMMA-CATCH Niger observation network (Galle et al., 2018; Lebel et al., 2009) with simulated precipitation under present and future climate conditions from the CP4-Africa convection-permitting simulation (Stratton et al., 2018; Senior et al., 2021). The methodology is then extended to the entire Sahel, for the first-time providing insight into future multi-duration extreme rainfall distributions over the region.

https://doi.org/10.5194/egusphere-2026-6628
Preprint. Discussion started: 30 October 2026
© Author(s) 2026. CC BY 4.0 License.

2 Theoretical framework and general methodology

2.1 IDF curves within the GEV simple scaling framework

In our study, the framework used to build IDF curves relies on the association of extreme value theory (EVT) with simple scaling theory. Within EVT, we adopt a block maxima analysis (BMA) for sampling extremes (Coles, 2001). Let I be the random variable associated with the annual maximum precipitation accumulation; i then denotes a value taken by I in its range of variation. In the context of BMA analysis, EVT asserts that for sufficiently large blocks, a sample of independent and identically distributed maxima converges in distribution to one of the generalized extreme value (GEV) distributions, whose cumulative distribution function F is:

$$F(i;\mu,\sigma,\xi) = \Pr(I \leq i) = \exp\left\{-\left[1+\xi\left(\frac{i-\mu}{\sigma}\right)\right]^{-1/\xi}\right\}, \quad \xi \neq 0,\ 1+\xi\frac{i-\mu}{\sigma} > 0 \tag{1}$$

where μ, $\sigma > 0$, and ξ are respectively the location, scale, and shape parameters. The first two parameters respectively control the location and the spread of the distribution around its center, while the shape parameter defines the behavior of the distribution tails. The intensity of a rainfall event with return period T, called the *return level* and denoted by $i(T)$, is then derived from the following equation:

$$i(T) = F^{-1}\left(1-\frac{1}{T}\right) \tag{2}$$

The classic approach to obtaining IDF curves consists of fitting a GEV distribution to annual maximum rainfall series for each duration and extracting the corresponding precipitation intensities for given return periods. This method has the advantage of being flexible but requires estimating $3 \times N$ parameters (N being the number of durations), which makes the process non-parsimonious and may affect the robustness of the IDF curve estimates (Chagnaud et al., 2023b). The simple scaling model, whose theoretical work was initiated by (Gupta and Waymire, 1990), and extensively used for deriving IDF curves, is based on the assumption of scale invariance, independent of return period, which implies similarity between precipitation distribution laws for different durations. Derived from fractal theory, the mathematical model used to describe the simple scaling property is:

$$I(D) \overset{d}{=} I(D_0)\left(\frac{D}{D_0}\right)^{\eta} \tag{3}$$

where D_0 is an arbitrary reference duration and $\overset{d}{=}$ means that there is equality between the statistical distribution of the reference values and that of the values scaled by the multiplicative factor. The parameter η ($\in [-1,0]$ when dealing with rainfall intensities) governs the slope of the decay of rainfall intensities with the duration of aggregation: the lower it is (close to -1), the stronger the decay. Combining Equations (2) and (3) gives a simple scaling GEV model (GEV-SS) that provides the return level for a given return period T and duration D:

https://doi.org/10.5194/egusphere-2026-6628
Preprint. Discussion started: 30 October 2026
© Author(s) 2026. CC BY 4.0 License.

$$i(T) = \left(\frac{D}{D_0}\right)^{\eta} \cdot F^{-1}\left(1 - \frac{1}{T}\right)$$
$$= \left(\frac{D}{D_0}\right)^{\eta} \left\{\mu_{D_0} + \frac{\sigma_{D_0}}{\xi}\left[\left(-\log\left(1 - \frac{1}{T}\right)\right)^{-\xi} - 1\right]\right\} \quad (4)$$

The GEV simple scaling model has the advantage of being more parsimonious, with only four parameters to adjust for a range of precipitation durations studied.

2.2 General framework for projecting intensity-duration-frequency curves from convection-permitting model

The method to project IDF curves relies on reference IDF curves derived from observations, as well as IDF curves simulated for present and future climates using a convection-permitting climate model with the GEV-SS model. The general principle of the proposed projection framework is schematically illustrated in Figure 1.

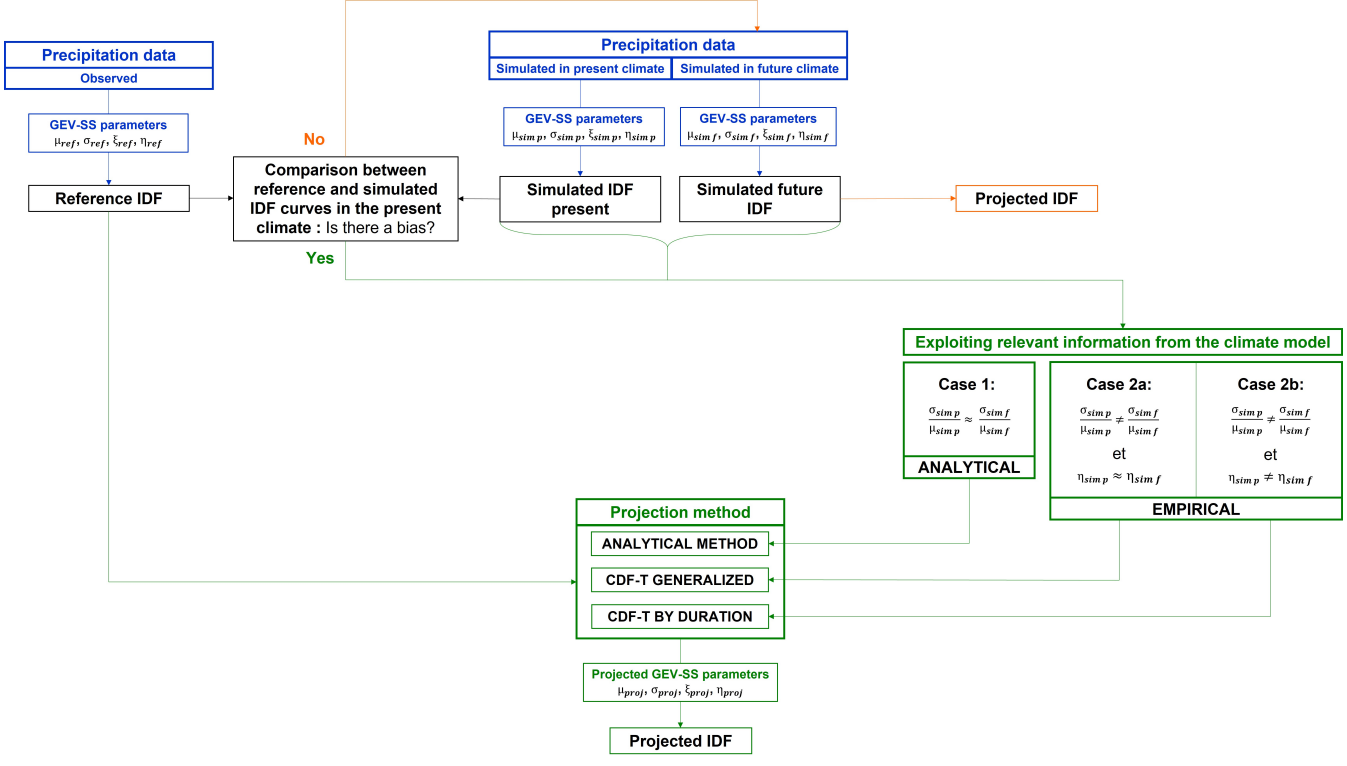

Figure 1. Schematic view of the methodology for projecting IDF curves. The red section is developed in this article. The symbols ≈ and ≠ used mean "not significantly different" and "significantly different" respectively.

The first step is to compare the reference IDF curves with the simulated IDF curves for the present climate in order to assess whether a bias exists, defined here as a systematic discrepancy between the reference and simulated IDF curves under present-

https://doi.org/10.5194/egusphere-2026-6628
Preprint. Discussion started: 30 October 2026
© Author(s) 2026. CC BY 4.0 License.

day conditions. In the absence of significant bias, the simulated future IDF curves can be directly considered as projected IDF curves. It should be noted, however, that the absence of bias in the present climate does not necessarily guarantee the absence of bias in future climates. Nevertheless, confidence in future projections is generally strengthened when the simulated present-day climatology exhibits limited bias.

When the simulated IDF curves exhibit significant bias, the second step consists of analyzing changes in the μ, σ, η, and η parameters of the GEV-SS model derived from CPM simulations.

In our approach, we seek to retain as much information as possible from the reference IDF curves, which are considered more robust than the simulated ones, while limiting the amount of information extracted from the convection-permitting model in order to minimize the influence of simulation biases.

To this end, we first focus on the evolution of the σ/μ ratio in the CPM simulations. Whether this ratio remains constant or changes between the present and future periods determines the projection framework to be adopted. Three cases can then be distinguished:

Case 1: $\frac{\sigma_{\text{sim } p}}{\mu_{\text{sim } p}} \approx \frac{\sigma_{\text{sim } f}}{\mu_{\text{sim } f}}$

The ratio σ/μ is not significantly different between the present and future simulated periods.

Assessing the assumption of a constant σ/μ ratio provides, on the one hand, a formal framework for projection, as will be shown below, and, on the other hand, reduces the number of parameters whose changes need to be estimated, thereby promoting a parsimonious projection framework. A constant σ/μ ratio implies that, even if extremes intensify, their relative variability remains stable. Consequently, for a given duration, all rainfall quantiles increase by the same proportion regardless of their return period. This is relevant information that can be used to project IDF curves within the theoretical framework of simple scaling. It is then possible to analytically project the parameter η without having to test its statistical constancy between the present and future climate simulated. We will refer to this first method as the analytical method, the assumptions of which are explained below:

- The projected location parameter μ is adjusted proportionally to the change in simulated location in the present and future periods, according to the following relationship:

$$\mu_{\text{proj}} = \frac{\mu_{\text{sim, future}}}{\mu_{\text{sim, present}}} \cdot \mu_{\text{ref}} \tag{5}$$

- The projected scale parameter σ is then calculated according to the constancy relationship σ/μ

$$\sigma_{\text{proj}} = \frac{\sigma_{\text{ref}}}{\mu_{\text{ref}}} \cdot \mu_{\text{proj}} \tag{6}$$

- The shape parameter ξ is assumed to be constant over time, derived from the reference IDF curves, as it is considered more robust.

https://doi.org/10.5194/egusphere-2026-6628
Preprint. Discussion started: 30 October 2026
© Author(s) 2026. CC BY 4.0 License.

– It is then possible to project the parameter η into the theoretical framework of simple scaling. Let us start from the following relationship, which links the location parameters for different precipitation durations:

$$\frac{\mu_{D,\text{ proj}}}{\mu_{D,\text{ ref}}} = \frac{\mu_{D,\text{ sim future}}}{\mu_{D,\text{ sim present}}} \tag{7}$$

The equations that define μ for the different cases are :

$$\mu_{D,\text{ proj}} = \left(\frac{D}{D_0}\right)^{\eta_{\text{proj}}} \cdot \mu_{\text{proj}} \tag{8}$$

$$\mu_{D,\text{ ref}} = \left(\frac{D}{D_0}\right)^{\eta_{\text{ref}}} \cdot \mu_{\text{ref}} \tag{9}$$

$$\mu_{D,\text{ sim future}} = \left(\frac{D}{D_0}\right)^{\eta_{\text{sim future}}} \cdot \mu_{\text{sim future}} \tag{10}$$

$$\mu_{D,\text{ sim present}} = \left(\frac{D}{D_0}\right)^{\eta_{\text{sim present}}} \cdot \mu_{\text{sim present}} \tag{11}$$

By expressing the ratios on both sides of the equations, we obtain:

$$\frac{\mu_{D,\text{ proj}}}{\mu_{D,\text{ ref}}} = \left(\frac{D}{D_0}\right)^{\eta_{\text{proj}}-\eta_{\text{ref}}} \cdot \frac{\mu_{\text{proj}}}{\mu_{\text{ref}}} \tag{12}$$

$$\frac{\mu_{D,\text{ sim future}}}{\mu_{D,\text{ sim present}}} = \left(\frac{D}{D_0}\right)^{\eta_{\text{sim future}}-\eta_{\text{ref}}} \cdot \frac{\mu_{\text{sim future}}}{\mu_{\text{sim present}}} \tag{13}$$

$$\left(\frac{D}{D_0}\right)^{\eta_{\text{proj}}-\eta_{\text{ref}}} \cdot \frac{\mu_{\text{proj}}}{\mu_{\text{ref}}} = \left(\frac{D}{D_0}\right)^{\eta_{\text{sim future}}-\eta_{\text{sim present}}} \cdot \frac{\mu_{\text{sim future}}}{\mu_{\text{sim present}}} \tag{14}$$

Hence :

$$\eta_{\text{proj}} = (\eta_{\text{sim future}} - \eta_{\text{sim present}}) + \eta_{\text{ref}} \tag{15}$$

Case 2: $\frac{\sigma_{\text{sim}\,p}}{\mu_{\text{sim}\,p}} \neq \frac{\sigma_{\text{sim}\,f}}{\mu_{\text{sim}\,f}}$

The ratio σ/μ is not significantly constant between the present and future simulated periods.

If this case, an empirical method, the CDF-t (Cumulative Distribution Function – transform) method can be applied for the

https://doi.org/10.5194/egusphere-2026-6628
Preprint. Discussion started: 30 October 2026
© Author(s) 2026. CC BY 4.0 License.

projection of IDF curves. Developed by (Michelangeli et al., 2009), the CDF-t method is based on the assumption that there is a transformation T that can translate the CDF of a simulated variable (in this case, temperature) into a CDF representing the climate variable observed locally by a given weather station (Figure 2). We define F_{ref} as the CDF derived from local data observed by a weather station for the historical period and $F_{\text{sim, present}}$ as the CDF of the simulated variable at the station location for the same period. F_{ref} and $F_{\text{sim, present}}$ are the CDFs equivalent to F_{proj} and $F_{\text{sim, future}}$ for the future period. Knowing $F_{\text{sim, future}}$, there exists a transformation T such that:

$$F_{ref}(x) = T(F_{sim,present}(x)) \tag{16}$$

We can then approximate the CDF F_{proj} by applying the transformation T to $F_{\text{sim, future}}$, which consists of first modeling T by replacing x with $F^{-1}_{\text{sim_present}}$. We then obtain the definition of T:

$$T(u) = F_{ref}(F^{-1}_{sim,present}(u)) \tag{17}$$

Therefore, assuming that $F_{proj}(x) = T(F_{sim,future}(x))$ is valid in the future, the CDF sought is provided by:

$$F_{proj}(x) = F_{ref}(F^{-1}_{sim,present}(F_{sim,futur}(x))) \tag{18}$$

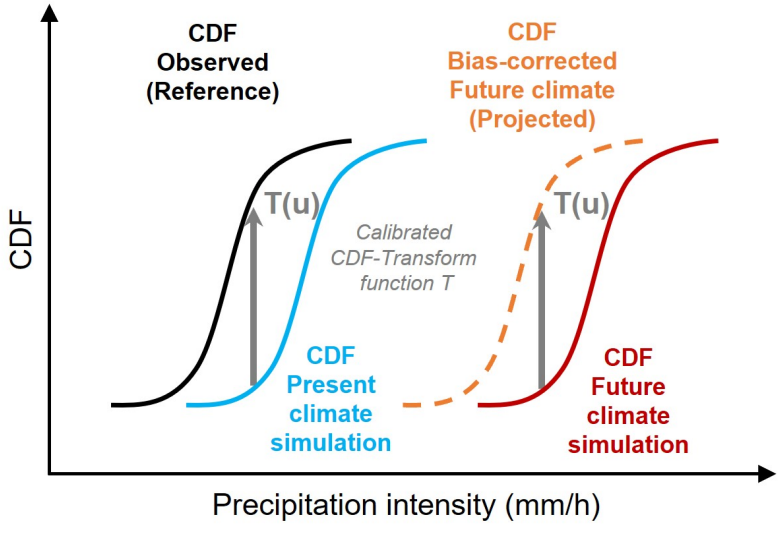

Figure 2. Schematic diagram showing the application of the CDF-t method.

In this article, applications of CDF-t were applied to empirical distributions, rather than to the GEV parameters themselves. Two distinct cases (case 2a and 2b) are identified for the application of the CDF-t depending on the constancy of the parameter η. A constant η means that the temporal scaling properties remain the same over time. In other words, the ratio of short-duration rainfall intensity to long-duration rainfall intensity remain stable over time. A constant η suggests that the physical structure of

https://doi.org/10.5194/egusphere-2026-6628
Preprint. Discussion started: 30 October 2026
© Author(s) 2026. CC BY 4.0 License.

extreme precipitation events (convective versus stratiform processes, storm organization) remains largely unchanged, implying that temporal scaling properties are preserved.

Case 2a: $\eta_{\mathrm{sim}\,p} \approx \eta_{\mathrm{sim}\,f}$

The parameter η is not significantly different between the present and future simulated periods. The method is applied using a generalized CDF-t approach, where a single transfer function T is calibrated from the normalized extreme rainfall distribution for all durations.

Case 2b: $\eta_{\mathrm{sim}\,p} \neq \eta_{\mathrm{sim}\,f}$

The parameter η is significantly different between the present and future simulated periods. The method is applied using a CDF-t by duration approach, in which a transfer function T is calibrated independently on the extreme rainfall distribution for each duration.

3 Case study description

3.1 West Africa Sahel context

The study focuses on the West African Sahel, defined here as the region bounded by 11°–17°N and 18°W–6°E (Figure 3). An intensification of the precipitation regime has been observed since the late 1980s. This evolution has been documented using both daily (Panthou et al., 2018) and sub-daily in-situ observations (Chagnaud et al., 2021), and has been largely attributed to anthropogenic climate forcing (Taylor et al., 2017; Chagnaud et al., 2023a). Combined with rapid population growth and high vulnerability to climate change, this intensification challenges hydrological risk managers to develop adequate adaptation strategies. The demand for climate services such as intensity–duration–frequency (IDF) curves is therefore high in the region (Amani and Paturel, 2017). This has led to recent research efforts on the topic (Bodian et al., 2016; Panthou et al., 2014a; Agbazo et al., 2016; Chagnaud et al., 2021), sometimes in direct collaboration with national meteorological services (Sane et al., 2018; Miller et al., 2022; Diedhiou et al., 2024).

3.2 Data

3.2.1 AMMA-CATCH Niger observed data

The AMMA-CATCH Niger (ACN) observatory, located in south-western Niger (between 1.6° and 3° E, and 13° and 14° N), has been documenting the evolution of the Sahelian rainfall regime since 1990, with high spatio-temporal resolution (Lebel et al., 2009). The observation network comprises 30 tipping bucket rain gauges, spread over an area of around 16,000 km^2 (Figure 3), providing rainfall timeseries with a timestep of 5 minutes for the period 1990-2019 (Galle et al., 2018). This in situ dataset, unrivalled in sub-Saharan Africa, provides a unique opportunity to characterize mean and extreme rainfall regimes at sub-daily scales. It has already supported research on IDF curves in the region (Panthou et al., 2014a; Chagnaud et al., 2021),

https://doi.org/10.5194/egusphere-2026-6628
Preprint. Discussion started: 30 October 2026
© Author(s) 2026. CC BY 4.0 License.

which confirmed the suitability of the assumptions underlying the GEV simple scaling framework used to develop the reference IDF curves in this study.

3.2.2 CP4-Africa climate model simulation

The CP4-Africa simulation is based on a convection-permitting, regional configuration of the Met Office Unified Model (UM) used for operational numerical weather prediction and whose physics and dynamics have been described in (Stratton et al., 2018). The simulation spans the African continent at horizontal grid spacing ranging from 4.4 km at the Equator to 3.2 km at 45S. Lateral boundary conditions are provided by a global atmospheric simulation performed with the Global Atmosphere 7.0 (GA7) configuration of the UM, with atmospheric concentration in ozone, aerosols and greenhouse gases typical of the 1990–2000 period (Stratton et al., 2018) to produce a 10-year simulation in present period (1997–2006). Sea surface temperatures (SSTs) are taken from Reynolds daily observations. The future simulation uses boundary conditions from the same global atmospheric simulation under RCP8.5 scenario, for a 10-year period around the end of the 21st century (2095-2104). SSTs are the sum of the SSTs used in the present-day simulations and the climatological average SST change between 1975–2005 and 2085–2115 in a HadGEM2-ES RCP8.5 run (Jones et al., 2011).

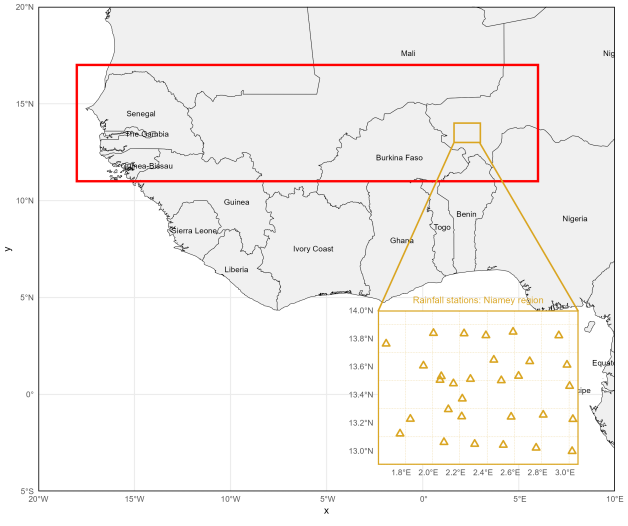

Figure 3. Map of West Africa with the western Sahel region outlined in red and the AMMA-CATCH Niger region with its rain gauges outlined in yellow.

3.3 Implementation

The methodology described in Section 2 is applied at both local and regional scales. The local-scale application illustrates, through a concrete case study, how the proposed projection framework can be implemented using reference IDF curves derived from present-climate observations. The availability of the AMMA-CATCH Niger rainfall dataset, in addition to the CP4-

https://doi.org/10.5194/egusphere-2026-6628
Preprint. Discussion started: 30 October 2026
© Author(s) 2026. CC BY 4.0 License.

Africa simulated rainfall data, enables the projection of reference IDF curves for the Niamey region. At the regional scale, the objective is to identify the most appropriate method for projecting IDF curves across the West African Sahel and to characterize the spatial patterns of change in GEV-SS model parameters inferred from CP4-Africa simulations. Each scale requires specific implementation choices, which are detailed below. In all cases, the CDF-t approach was implemented using the CDFt R package.

3.3.1 In a local context

- **Extreme rainfall sampling:** The series of annual maxima were constructed using rainfall data recorded every 5 minutes (AMMA-CATCH) and simulated every hour (CP4-Africa), applying a moving average over windows ranging from 2 to 24 hours. (Panthou et al., 2014b) showed that the invariance property of the parameter η applies to AMMA-CATCH data in Niger for durations between 1 and 24 hours, although a deviation is observed for $D = 1$ hour. Given that the time step of the CP4-Africa simulations is hourly, this assessment focuses on durations ranging from 2 to 24 hours. Applying a sliding window smooths the data and avoids fragmentation of rainfall events. For each duration considered, the sliding annual maxima are extracted, thus producing, for each station, m vectors of length N, corresponding to the annual maxima, where m is the number of durations ($D \in \{2, 4, 6, 12, 24\ \text{h}\}$) and N is the number of available years.

- **Pooling approach:** In order to reduce sampling variance, the 30 rainfall stations were grouped together in a regional sample. This approach is justified by the nature of rainfall extremes in the region, which are mainly linked to convective systems with a short lifespan and limited spatial extent. As a result, annual maximum series generally show low spatial correlation, much lower than that observed for annual totals. The stations can therefore be considered as sampling the same regional population of precipitation extremes (as already demonstrated in (Chagnaud et al., 2021). The regional sample obtained takes the form of a matrix with m columns (the different durations) and $N \times q$ rows (where q is the number of stations), each corresponding to an observation of a sliding annual maximum. The pooling approach was also applied to CP4-Africa rainfall data for both present and future periods by selecting the 30 pixels located at the AMMA-CATCH stations (Figure 4).

3.3.2 In a regional context

- **Assessment of GEV-SS parameters:** The GEV-SS parameters $\{\mu, \sigma, \xi, \eta\}$ for precipitation data from the climate model for the present and future climate were calculated by grouping precipitation data using sliding windows centered on each pixel. Each window covers 5×5 pixels i.e., 20 km x 20 km, excluding border effects. This approach has increased the robustness of GEV parameter estimates by providing 250 sampled precipitation values over 10 years of present and future climate data, respectively (Figure 5a). As a result, GEV parameter estimates are much more coherent in space, compared to a more noisy pixel by pixel approach that reflects sampling effects (not shown).

- **Assessment of the significance of changes in GEV-SS parameters:** The significance of the constancy of the σ/μ ratio and the η parameter between the present and future periods of the climate model were assessed using the Wilcoxon

https://doi.org/10.5194/egusphere-2026-6628
Preprint. Discussion started: 30 October 2026
© Author(s) 2026. CC BY 4.0 License.

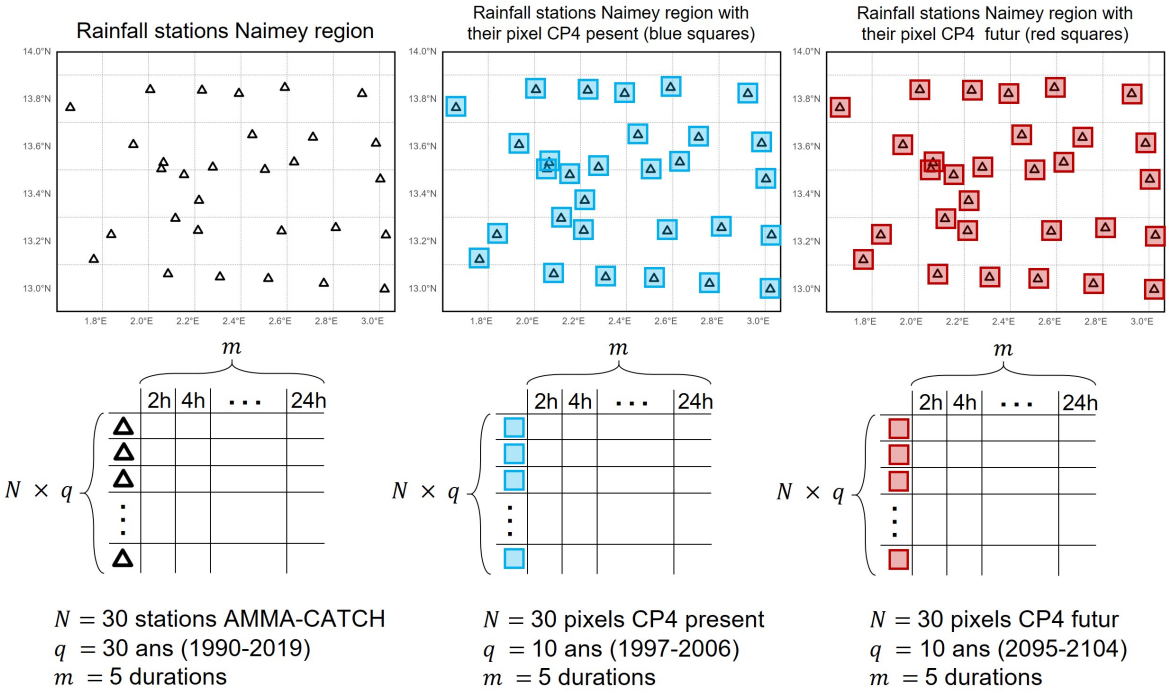

Figure 4. Schematic view of the pooling approach for the AMMA-CATCH, CP4 present and CP4 futur extreme rainfall sampling.

test, a nonparametric test based on median values (Figure 5b). Its null hypothesis (H0) corresponds to the absence of a significant difference in the the median between the present period and the future period, while the alternative hypothesis (H1) assumes the existence of a significant difference between the medians of these two periods, with a 5% risk of error. The Wilcoxon test was applied to precipitation data sets defined using sliding windows centered on each pixel of the CP4-Africa climate model. To combine statistical robustness and test power with climatological considerations, we used a sliding window of 25×25 pixels, i.e., 100 km x 100 km. From these pixels, only the 10% farthest apart were selected for the test, to limit spatial dependencies. From a statistical point of view, this choice provides a sufficient number of data points that can be considered independent. In terms of climate, it is consistent with the spatial scale of mesoscale convective systems, which are the main contributors to the precipitation studied (Mathon et al., 2002).

https://doi.org/10.5194/egusphere-2026-6628
Preprint. Discussion started: 30 October 2026
© Author(s) 2026. CC BY 4.0 License.

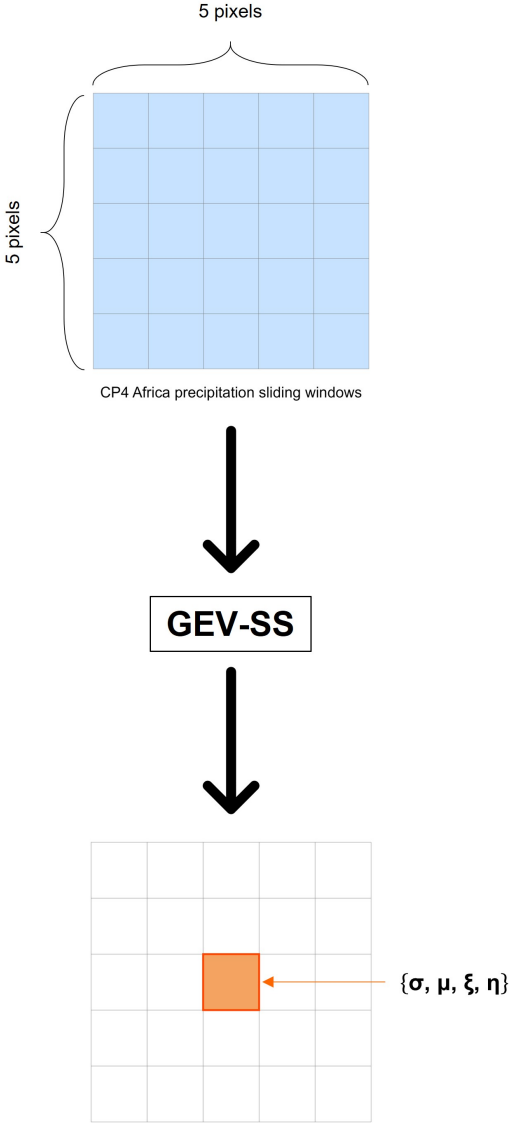

(a) Schematic diagram of the GEV parameters estimation for a centered pixel based on a sliding window of 5×5 pixels, i.e., 25 precipitation pixels.

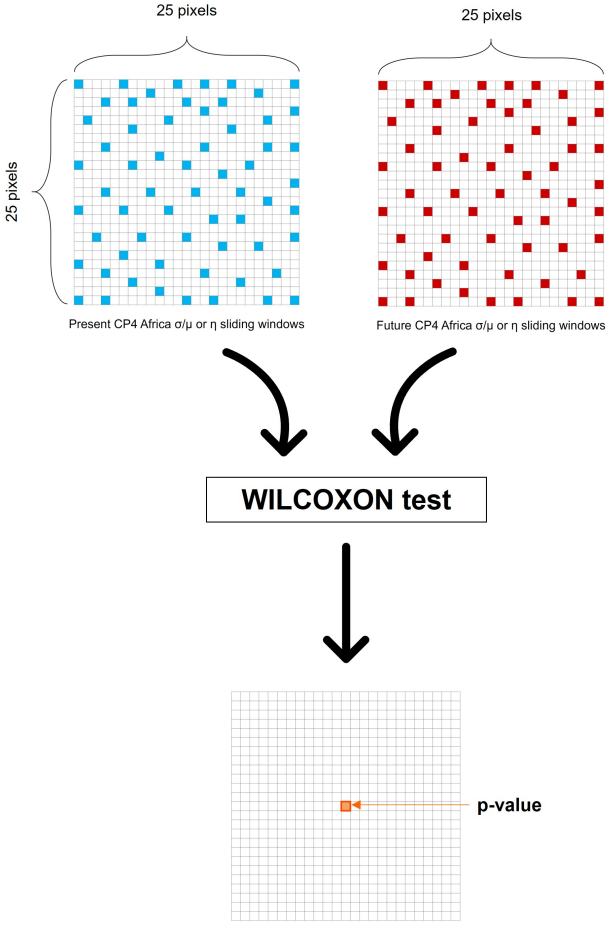

(b) Schematic diagram of the Wilcoxon test applied pixel by pixel using sliding windows of 25×25 pixels (625 pixels). For each central pixel, the test compares the values at the same spatial coordinates between present CP4 (in blue) and future CP4 (in red), considering only the 10% of pixels furthest from the window, i.e., 63 pixels. This analysis is performed for the σ/μ ratio and for the η parameter. For each pixel, the test result is expressed by the associated p-value.

Figure 5. Schematic diagram of the assessment of GEV parameters and the Wilcoxon test.

https://doi.org/10.5194/egusphere-2026-6628
Preprint. Discussion started: 30 October 2026
© Author(s) 2026. CC BY 4.0 License.

4 Results

4.1 Projection of IDF curves: application case study in the Niamey region of Niger

4.1.1 Assessment of CP4-Africa precipitation in the current climate in the Niamey region (AMMA-CATCH Niger)

The first step is to determine whether the rainfall data show any bias by comparing the maximum annual reference intensities with those simulated in the current climate by the CP4-Africa model. In this context, IDF curves serve as a tool for assessing local climatology. Table 1 shows the GEV parameters for AMMA-CATCH for each of the three periods (1990-1999, 2000-2009 and 2010-2019) and for CP4-Africa present. Figure 6 shows the IDF curves for the 10-year and 100-year return periods for:

- The reference climate in the AMMA-CATCH zone over three 10-year periods: 1990-1999, 2000-2009, and 2010-2019 ;
- The climate simulated for the present period by the CP4-Africa model (1997-2006). Simulated precipitation data were extracted at pixels corresponding to the locations of AMMA-CATCH stations.

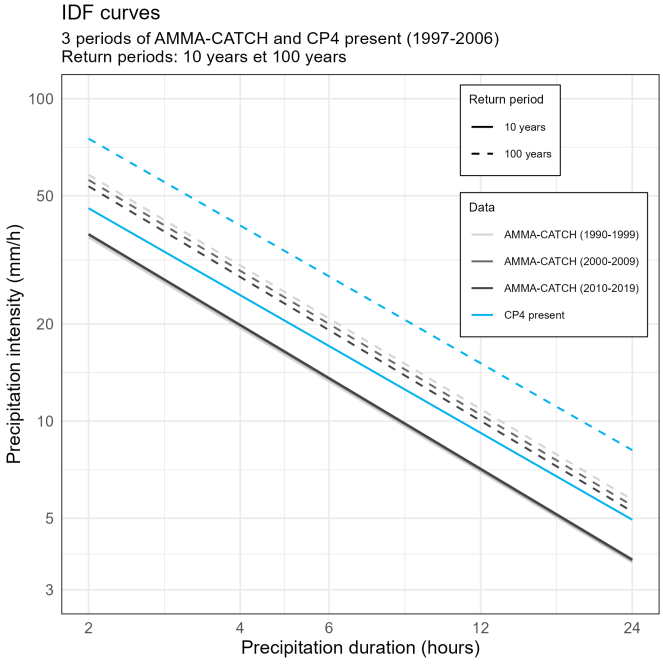

Figure 6. IDF curves for the three 10-year periods of AMMA-CATCH (1990-1999, 2000-2009, and 2010-2019) and for CP4 present (1997-2006) for return periods of 10 years and 100 years.

The results of the IDF curves show a bias in precipitation data between the observed AMMA-CATCH data (3 periods of 10 years) and the simulated CP4-Africa data in the present climate (1997-2006). The CP4-Africa climate model with a resolution

https://doi.org/10.5194/egusphere-2026-6628
Preprint. Discussion started: 30 October 2026
© Author(s) 2026. CC BY 4.0 License.

of 4.5 km tends to overestimate precipitation intensities. This finding is consistent with what is described in the CP4-Africa guide (Senior et al., 2020): if CP4-Africa is analyzed on its native 4.5 km grid, precipitation is generally too intense (low precipitation rates are underestimated and high rates are overestimated), for example in July-August in the Sahel (Berthou et al., 2019).

4.1.2 Selection of the projected method for the Niamey region case study (AMMA-CATCH Niger)

The method described in Section 2 involves identifying the specific case in order to select the most appropriate approach for projecting IDF curves. Based on the p-values obtained from the Wilcoxon test applied at the scale of the West African Sahel (Figure 11a), the σ/μ ratio appears to be constant in the Niamey region regarding the pixels of CP4-Africa corresponding to the rainfall stations of the AMMA-CATCH Niger network. Only 3 out of 30 stations are located on pixels with a p-value lower than the 5% threshold and 85% of the AMMA-CATCH area has a non-significant σ/μ ratio (Figure 7, zoom from Figure 11a). Since the IDF curves are derived from pooled rainfall data, the application of the analytical method for their projection in the Niamey region appears justified.

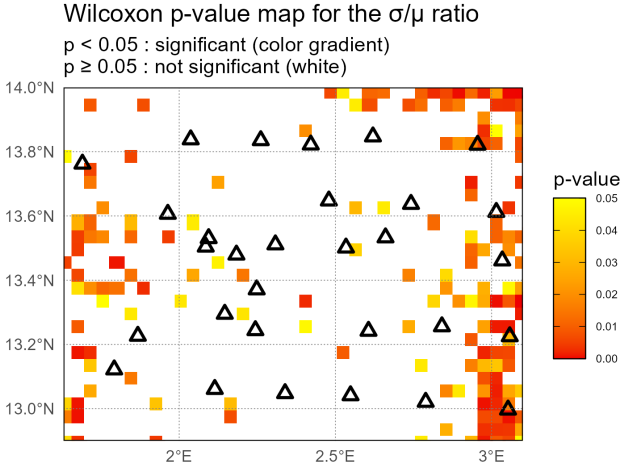

Figure 7. Results of the Wilcoxon test p-values for the AMMA-CATCH region for the σ/μ ratio. The black triangles represent the rain gauge stations of the AMMA-CATCH Niger network.

Table 1 provides the GEV parameters obtained for CP4 present and future, as well as for the analytical method, and those corresponding to the reference IDF curves. Figure 8a illustrates the reference IDF curves, and those derived from the CP4-Africa model for present and future climates. Figure 8b shows the IDF curves projected for the AMMA-CATCH Niger area with the analytical method. Projections indicate a significant reduction in return periods (Figure 8b): an event with an estimated return period of 100 years under the reference climate would now correspond to a return period of approximately 10 years in the future climate.

https://doi.org/10.5194/egusphere-2026-6628
Preprint. Discussion started: 30 October 2026
© Author(s) 2026. CC BY 4.0 License.

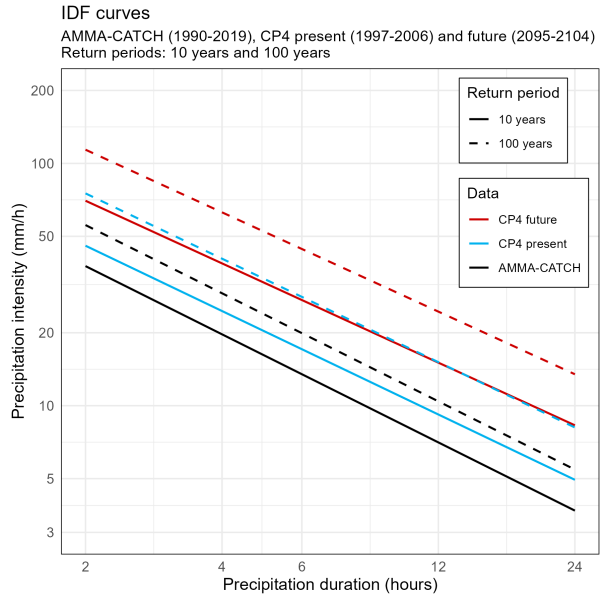

(a) Reference (in black), present CP4 (in blue), and future CP4 (in red).

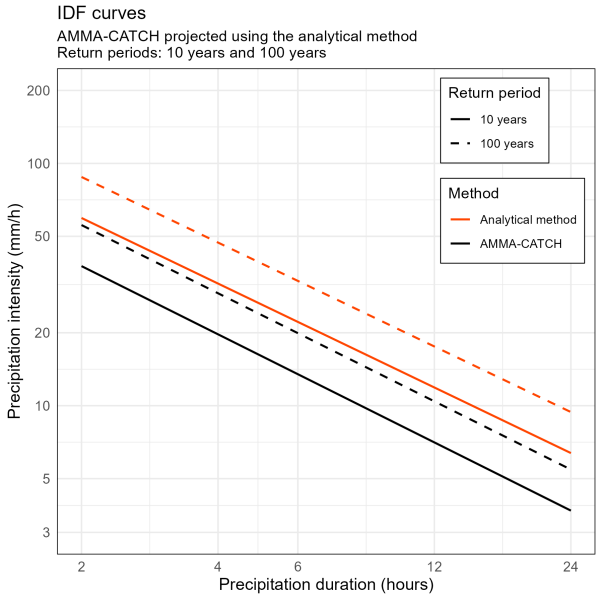

(b) Reference (in black) and projected using the analytical method (in orange).

Figure 8. IDF curves of 10 years (solid line) and 100 years (dashed line).

4.1.3 Sensitivity among the three projection methods for the Niamey region case study (AMMA-CATCH Niger)

Although the analytical method is suitable for projecting IDF curves onto the Niamey region, in this section we will examine how the projected IDFs vary to the choice of method. Table 1 provides the GEV law parameters obtained for each of the projection methods, and those corresponding to the reference IDF curves. Figure 9 shows the IDF curves projected for the AMMA-CATCH Niger area according to the three approaches considered: the analytical method, the generalized CDF-t, and the CDF-t duration by duration.

The results show a strong similarity between the projected IDF curves obtained by the three methods for the AMMA-CATCH area. The relative difference between these methods, calculated in relation to the projected average intensities, is around 10% or less depending on the duration of precipitation. In comparison, the difference between the reference intensities and the projected average intensities reaches values between 35% and 40%, depending on the duration considered.

The similarity of the results obtained with the three methods is reassuring. It shows that, in cases where the change in the σ/μ ratio between present and future climates is not statistically significant, an empirical approach does not substantially degrade the quality of the projections. However, it should be noted that the analytical method proposed here is preferable, as it is more parsimonious and consequently more robust.

https://doi.org/10.5194/egusphere-2026-6628
Preprint. Discussion started: 30 October 2026
© Author(s) 2026. CC BY 4.0 License.

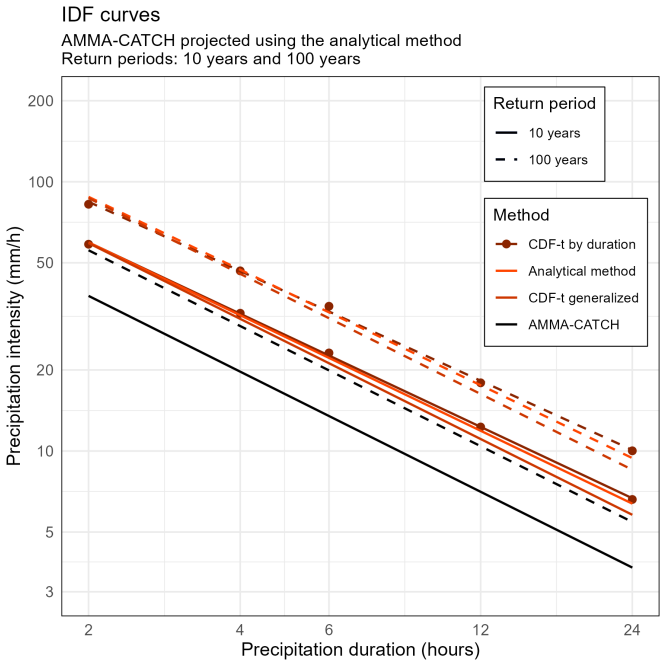

Figure 9. IDF curves AMMA-CATCH (1990-2019) and projected using the tree methods for return periods of 10 years and 100 years.

4.2 Regional mapping of IDF projection methods in the Sahel

The generic framework offers three methods (analytical, generalized CDF-t, CDF-t duration by duration), the choice of which is determined by the constancy of the σ/μ ratio and η parameter between present and future CP4 simulations. Figure 10 shows the μ, σ, and η parameters and σ/μ ratio for the CP4-Africa model under present and future climate conditions, as well as their relative differences across the West African Sahel. The μ and σ parameters show latitudinal gradients (Figures 10a and 10b) consistent with what is known about the region's climatology (Panthou et al., 2012). The relative difference in the σ/μ ratio is particularly pronounced over Senegal (Figure 10i). The relative difference in the η parameter (Figure 10l) does not show any particular spatial distribution.

We then applied the Wilcoxon test to determine whether these differences were statistically significant, in particular for the σ/μ ratio and the η parameter (Figures 11a and 11b). The results indicate that the η parameter differs significantly across the Sahel between the present and future climates simulated by CP4-Africa, without showing any particular spatial structure. On the other hand, for the σ/μ ratio, some areas are characterized by insignificant differences, reflecting a relatively constant ratio, particularly around the Niamey region (AMMA-CATCH area outlined in red in the figures), in Burkina Faso and central Mali.

By combining the two significance maps, we obtain a summary map that identifies the most appropriate projection method for each geographical area in the Sahel West African (Figure 12).

https://doi.org/10.5194/egusphere-2026-6628
Preprint. Discussion started: 30 October 2026
© Author(s) 2026. CC BY 4.0 License.

IDF curves	μ	σ	ξ	η	σ/μ
CP4 present (1997-2006)	23.94	8.51	0.11	-0.90	0.36
CP4 future (2095-2104)	37.82	12.6	0.11	-0.86	0.33
Reference AMMA-CATCH (1990-2019)	22.94	6.07	0.07	-0.94	
AMMA-CATCH (1990-1999)	22.16	5.73	0.13	-0.93	
AMMA-CATCH (2000-2009)	23.11	6.02	0.07	-0.94	—
AMMA-CATCH (2010-2019)	23.58	6.37	0.01	-0.94	
Projected with analytical method	36.25	9.58	0.07 (reference value)	-0.90	
Projected with CDF-t generalized	37.74	8.55	-0.09	-0.94 (reference value)	
Projected with CDF-t by duration	37.77 | 2h	8.85 | 2h	0.04 | 2h	-0.88 | 10 ans	
	21.31 | 4h	4.51 | 4h	0.08 | 4h	-0.85 | 100 ans	
	14.91 | 6h	3.17 | 6h	0.12 | 6h		
	7.93 | 12h	1.74 | 12h	0.09 | 12h		
	4.13 | 24h	0.96 | 24h	0.12 | 24h		

Table 1. GEV parameters for IDF curves (CP4 present, CP4 future, Reference AMMA-CATCH, AMMA-CATCH with 3 periods: 1990–1999, 2000–2009 and 2010–2019) and projected IDF curves using the three methods (Analytical method, CDF-t generalized and CDF-t by duration).

The principle adopted is as follows: when the condition for applying the analytical method is not satisfied, i.e., the assumption of constancy of the σ/μ ratio, an empirical approach must be used, in this case the CDF-t method. The CDF-t method can be broken down into two approaches — "generalized" and "by duration" — depending on whether the parameter η can be considered constant or not. The constancy of this parameter, which reflects an invariance in the relationship between the

https://doi.org/10.5194/egusphere-2026-6628
Preprint. Discussion started: 30 October 2026
© Author(s) 2026. CC BY 4.0 License.

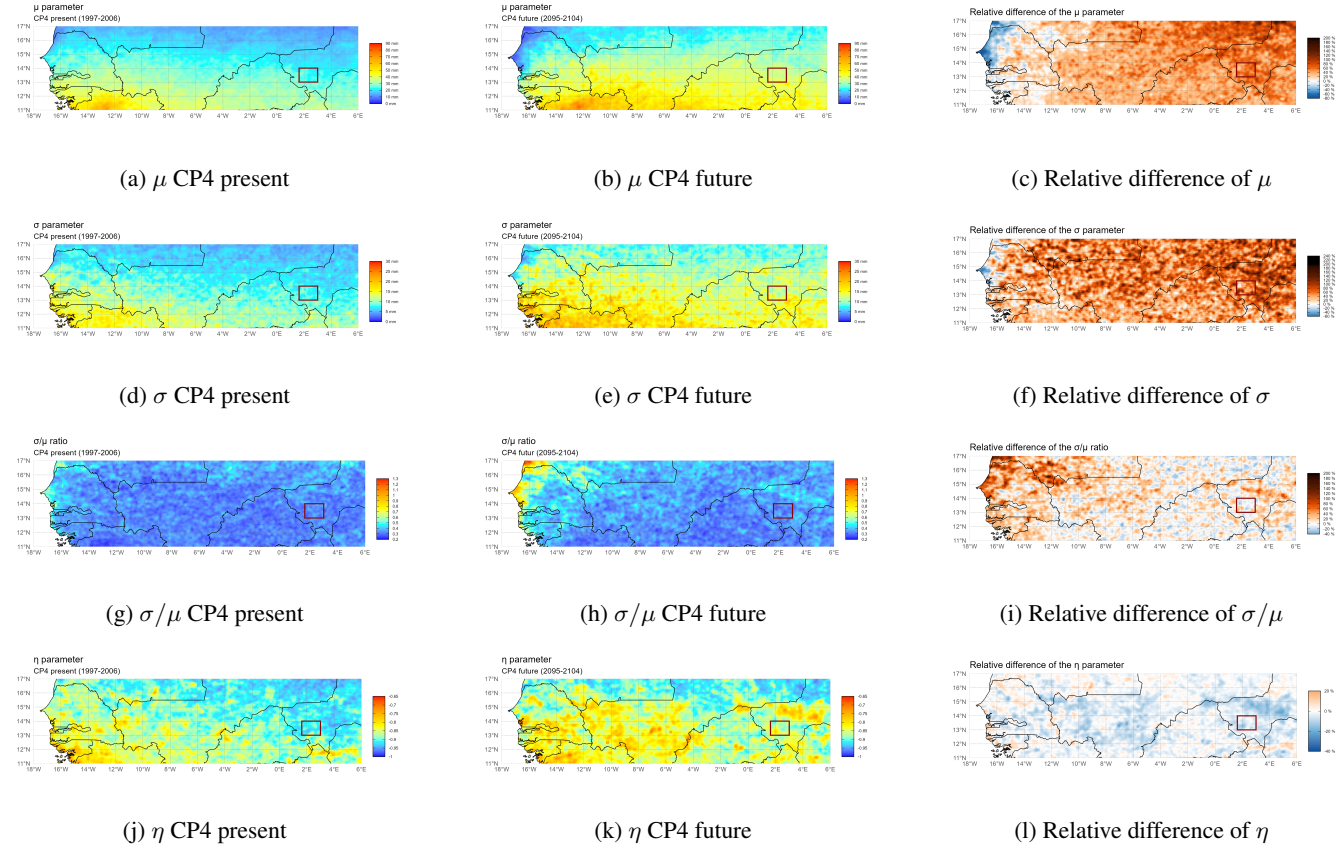

(a) μ CP4 present (b) μ CP4 future (c) Relative difference of μ

(d) σ CP4 present (e) σ CP4 future (f) Relative difference of σ

(g) σ/μ CP4 present (h) σ/μ CP4 future (i) Relative difference of σ/μ

(j) η CP4 present (k) η CP4 future (l) Relative difference of η

Figure 10. GEV parameters μ, σ, η parameters and σ/μ ratio, for CP4 present and future and their relative difference. The dark red area outlines the AMMA-CATCH region of Niger.

intensity and duration of rainfall events, suggests that the physical structure of convective systems (spatial and temporal pattern, size and propagation speed) remain unchanged.

The analytical method (σ/μ ratio significantly constant) covers 49% of the region. The CDF-t method by duration (σ/μ ratio and parameter η not significantly constant) covers 38% of the territory while the generalized CDF-t method (σ/μ ratio not significantly constant and parameter η significantly constant) remains marginal, with only 13% coverage. A spatial trend also seems to be emerging, with the analytical method predominating in the southern to southeastern and northeastern part of the Sahel. The AMMA-CATCH Niger zone is mainly associated with this method. However, in Senegal, the use of empirical methods (generalized CDF-t or CDF-t by-duration) is largely dominant, which could suggest specific changes in the physical mechanisms underlying convective systems in the future in this country. This will be discussed in more detail in section 5.

https://doi.org/10.5194/egusphere-2026-6628
Preprint. Discussion started: 30 October 2026
© Author(s) 2026. CC BY 4.0 License.

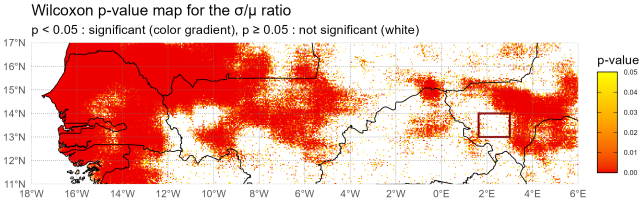

(a) Wilcoxon p-value map for the σ/μ ratio

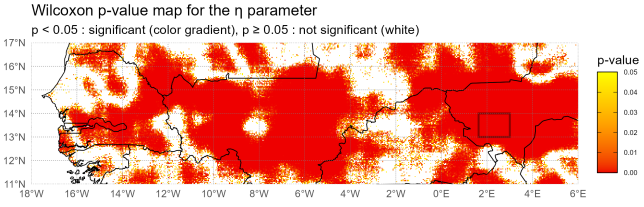

(b) Wilcoxon p-value map for the η parameter

Figure 11. Results of the Wilcoxon test p-values for the Sahel region for the σ/μ ratio (11a) and η (11b) parameters. The dark red area outlines the AMMA-CATCH Niger region.

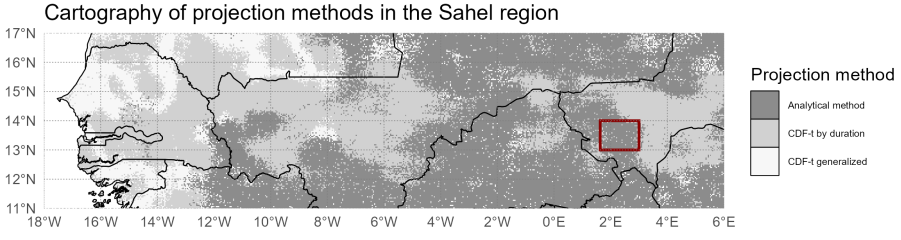

Figure 12. Cartography of projection methods in the Sahel region : Analytic method, CDF-t generalized and CDF-t by duration. The dark red box delimits the AMMA-CATCH Niger region.

https://doi.org/10.5194/egusphere-2026-6628
Preprint. Discussion started: 30 October 2026
© Author(s) 2026. CC BY 4.0 License.

5 Discussions

5.1 Changes in GEV parameters and future climatology

The maps in Figure 10 highlight distinct patterns in the evolution of GEV distribution parameters between present and future climates. The potential relationship between these regional changes in extreme value distributions and the mean precipitation regime is examined here.

The extreme value theory shows under certain assumptions (Coles, 2001; Madsen et al., 1997; Panthou et al., 2014a) that the μ parameter depends on the combined effect of the average occurrence of precipitation and its average intensity, while σ depends mainly on the average intensity.

Figures 13a and 13b show the relative differences in daily rainfall occurrence and intensity simulated by CP4. The maps exhibit spatial patterns consistent with those reported in the literature on climate projections for the West African Sahel (Chagnaud et al., 2023a; Sow et al., 2025; Monerie et al., 2020). They highlight a widespread intensification of precipitation, reflected primarily in a marked increase in the average intensity of daily rainfall, with the exception of the western tip of Senegal. In addition, changes in the occurrence of daily rainfall are also observed, revealing contrasting trends at the regional level: a gradual increase in occurrence appears towards the northeast of the region, while a more pronounced decrease is observed in the western part of the study area.

These changes in mean climatology are also reflected in the spatial patterns of relative differences in the GEV distribution (Figures 10c and 10f). The relative difference map for the μ parameter shows stronger increases in the northeast of the region and fairly marked decreases in the west. The relative difference map for the σ parameter shows a general increase across the region except for the far west.

Given the spatial pattern on the σ and μ maps, the increase in the σ/μ ratio visible in the western part of the study area might therefore be attributed to this significant change in average rainfall intensity at the regional scale. When this regional intensification signal is superimposed on east-west gradients controlled mainly by occurrences, the σ/μ ratio changes little or even decreases, as is the case over most of the center and east of the region. However, some spatial pattern of increases in the σ/μ ratio are still visible, which prevents us from being entirely certain about this observation (Figure 10i). At present, it is difficult to estimate whether these are sampling effects or local changes in climatology.

The question of robustness also arises when attempting to analyze the climatological reasons that could explain changes in the η parameter. The dominant spatial distribution shows a decrease in the η parameter (Figure 10l). This decrease could be analyzed as a temporal persistence of convection, larger or slower convective systems. It is difficult to draw conclusions about such hypotheses here. This is particularly true given that sampling effects and possible parameter compensation in the GEV-SS model may interfere with the spatial pattern of the η parameter.

https://doi.org/10.5194/egusphere-2026-6628
Preprint. Discussion started: 30 October 2026
© Author(s) 2026. CC BY 4.0 License.

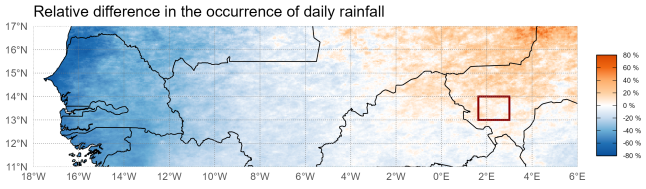

(a) Relative difference of the occurrence of daily rainfall

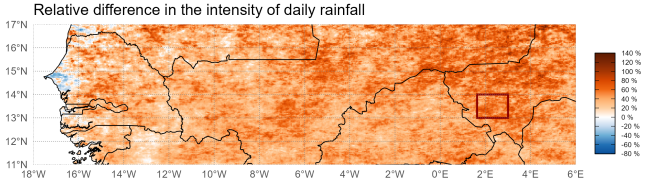

(b) Relative difference of the intensity of daily rainfall

Figure 13. Relative difference of occurrence and intensity daily rainfall between CP4 future and present. The dark red area outlines the AMMA-CATCH region of Niger.

5.2 The limitations of the method

5.2.1 Uncertainties affecting IDF curve projections

Several sources of uncertainty affect the projection of extreme precipitation. The first one arises from the statistical fitting of IDF curves. This could be assessed using bootstrap techniques (Chagnaud et al., 2021). Although such tehcniques are useful for the operational use of IDF curves (Sane et al., 2018; Chagnaud et al., 2021), they are not evaluated here, as their contribution to overall uncertainty is assumed to be minor compared to other sources (Zhao et al., 2022). The other sources of uncertainty arise from climate simulations. First, CP4-Africa is forced by a single global climate model (GA7 from the MetOfffice). Moreover, only one greenhouse gas concentration scenario is used, the RCP 8.5 scenario, whose probability now seems reduced in view of current policies. Finally, the simulation is based on a single ensemble member. This last point poses the following question: does CP4-Africa simulate a drier or wetter trajectory of possible climate variability? In the absence of a set of simulations, internal climate variability is not represented. All these limitations prevent the construction of uncertainty intervals around the projected IDF curves. The CP4-Africa model is primarily an opportunity to apply our methodology, as its fine spatial resolution (4 km) is compatible with AMMA-CATCH reference data. However, it does not allow us to establish a plausible range of projected IDF curves for the future and the projected IDF curves presented here cannot be considered as reliable projections for operational use.

https://doi.org/10.5194/egusphere-2026-6628
Preprint. Discussion started: 30 October 2026
© Author(s) 2026. CC BY 4.0 License.

5.2.2 Wilcoxon test to assess the significance of the σ/μ ratio and η parameter

The significance results for the σ/μ ratio and the η parameter may be sensitive to the size of the window considered and the size of the sample it contains. For the AMMA-CATCH region, this sensitivity does not have an impact on the projections of the IDF curves, which turned out to be very similar across the three methods. However, in other regions of the world, a question may be posed: is the Wilcoxon test sufficiently powerful to assess the significance of the consistency of the σ/μ ratio and η parameter? Other statistical tests, such as the Student's t-test, could be used to assess the significance of the ratio and eta parameters. The classic 5% p-value threshold is an arbitrary choice that could also be adjusted. An ad hoc method could be considered in order to obtain a more robust assessment of the significance of changes in the ratio and eta parameters, similar to the approach proposed by (Chagnaud et al., 2021) for detecting trends in GEV parameters. This methodological approach could enable more reliable diagnoses to be made, particularly in regions where climatic contrasts or sample sizes make the Wilcoxon test less discriminating.

5.2.3 Using the CDF-t method

The CDF-t method was chosen to address the need to project the multi-scale distribution of extremes within an empirical framework that preserves CPM bias characteristics. Its main advantage is that it is non-parametric and thus directly driven by the data. It has also several limitations. First, it is sensitive to the quality of the observed data. In the case of AMMA-CATCH, we have a continuous 30-year series of very high-quality precipitation data, which makes the application of this method particularly relevant. An alternative approach, particularly when data availability is limited, relies on directly estimating relative changes in IDF curve parameters from CPM simulations and applying these changes to reference IDF curves. This method, as proposed for example by (Cannon and Innocenti, 2019), implicitly assumes that model biases cancel out in relative space, which is debatable. The CDF-t method is also based on the assumption of stationarity of distributions. This assumption can be considered reasonable for the 10-year periods of the CP4 model, for both the present and future climate. However, for the 30 years of AMMA-CATCH reference data, (Chagnaud et al., 2021) have shown significant non-stationarity in the parameters of the GEV distribution. Usually, a trend removal step is applied to the data before using the CDF-t method in order to satisfy the stationarity assumption. In this study, we do not remove the trend, as our focus is on the projection of reference IDF curves rather than on the development of non-stationary reference curves. The extension of our framework to non-stationary IDF curves could be envisaged, but lies beyond the scope of this study.

6 Conclusion

The presented study has allowed us to propose a generic methodological framework for the projection of multi-scale extreme value distributions. This approach can be transferred to any region for which reference series and two simulated precipitation periods are available—representing the current climate and the future climate, respectively, and with spatial resolution compatible with the reference data. The analysis focused on extracting information from CPMs by regarding the GEV-SS parameters.

https://doi.org/10.5194/egusphere-2026-6628
Preprint. Discussion started: 30 October 2026
© Author(s) 2026. CC BY 4.0 License.

In this case, the constancy of the σ/μ ratio and η parameter, were evaluated using the Wilcoxon test, in order to determine the most appropriate method for projecting IDF curves. This resulted in three methodological configurations:

- **Case 1:** a significantly not different σ/μ ratio, leading to the formulation of an analytical method to project IDF curves.

If the σ/μ ratio proves to be significantly different, then we turn to an empirical method, in this case the CDF-t method. Two cases are then possible:

- **Case 2a:** a significantly not different η parameter, justifying the application of the generalized CDF-t;
- **Case 2b:** a significantly different η parameter, implying the use of the CDF-t by duration.

In our study the methodological framework was applied to the West African Sahelian context using CP4-Africa simulations and the high-resolution rainfall dataset AMMA-CATCH Niger in the Niamey region.

At the local scale of the Niamey region, the σ/μ ratio is considered constant, based on the Wilcoxon test applied at the regional scale, which implies using the analytical method to project the distributions of precipitation extremes, represented by the IDF curves. The sensitivity to the three methods was also examined for this region and shows a high degree of similarity between the results (order of 10%).

At the regional scale, the results of the Wilcoxon tests for the σ/μ ratio and the η parameter also enabled the three methods to be mapped across the West African Sahel. The analytical method (Case 1) covers 49% of the region, the CDF-t by duration method (Case 2b) covers 38% of the territory, while the generalized CDF-t method (Case 2a) remains marginal, with only 13% coverage. The regional study also made it possible to characterize changes in the parameters of the GEV-SS model. Both the local and regional analyses provide additional insights into the climatological interpretation of the results. At the local scale, the projection of IDF curves over the Niamey region suggests that an event associated with a 100-year return period under present-day conditions could correspond to a return period of approximately 10 years under the future climate simulated by CP4-Africa. At the regional scale, coherent spatial patterns emerge in the evolution of multi-scale extreme value distribution parameters. These patterns are consistent with the projected changes in the mean precipitation regime, suggesting a degree of physical consistency between changes in mean and extreme precipitation characteristics. These results should nevertheless be interpreted with caution, given the limitations associated with the CP4-Africa experimental design discussed in this study, in particular the limited number of simulated years and the dependence on a single global forcing configuration. The increasing availability of CPM-based simulations at continental and global scales is expected to provide a more robust basis for assessing the robustness and uncertainty of these findings. The methodological framework proposed in this study is intended to contribute to this effort. It is transferable to other CPM datasets and can be applied in other hydro-climatic regions beyond the present West African case study.

Data availability. CP4-Africa is a high-resolution regional climate model simulation as part of the Future Climate for Africa (FCFA) program. Its precipitation data are accessible from the website (Centre for Environmental Data Analysis (CEDA), 2018).

https://doi.org/10.5194/egusphere-2026-6628
Preprint. Discussion started: 30 October 2026
© Author(s) 2026. CC BY 4.0 License.

Author contributions. LM, YS, GP and TV conceived the idea. LM carried out the analysis, and whote the article. TV, GP, TL and GC particpated in the discussion and design of this study and contribued to wrriting and editing the paper. YS also particpated in editing the paper.

Competing interests. The authors declare there are no conflicts of interest for this manuscript.

Acknowledgements. Laura Marimbordes, Théo Vischel, Geremy Panthou and Thierry Lebel are supported by the AFD/IRD CECC project. The authors thank Romain Barbier for the final formatting of the manuscript.

https://doi.org/10.5194/egusphere-2026-6628
Preprint. Discussion started: 30 October 2026
© Author(s) 2026. CC BY 4.0 License.

References

Agbazo, M. N., Koto N'Gobi, G., Kounouhewa, B., Alamou, E., Afouda, A., and Akpo, A.: Estimation of IDF Curves of Extreme Rainfall by Simple Scaling in Northern Oueme Valley, Benin Republic (West Africa), 20, 1–7, https://doi.org/10.15446/esrj.v20n1.49405, 2016.

Allan, R. P., Barlow, M., Byrne, M. P., Cherchi, A., Douville, H., Fowler, H. J., Gan, T. Y., Pendergrass, A. G., Rosenfeld, D., Swann, A. L. S., Wilcox, L. J., and Zolina, O.: Advances in understanding large-scale responses of the water cycle to climate change, 1472, 49–75, https://doi.org/10.1111/nyas.14337, 2020.

Allen, M. R. and Ingram, W. J.: Constraints on future changes in climate and the hydrologic cycle, 419, 224–232, https://doi.org/10.1038/nature01092, 2002.

Amani, A. and Paturel, J.-E.: Le projet de révision des normes hydrologiques en Afrique de l'Ouest et Afrique Centrale, p. 6, https://doi.org/10.4267/2042/61964, 2017.

Ban, N., Schmidli, J., and Schär, C.: Evaluation of the convection-resolving regional climate modeling approach in decade-long simulations, 119, 7889–7907, https://doi.org/10.1002/2014JD021478, 2014.

Ban, N., Schmidli, J., and Schär, C.: Heavy precipitation in a changing climate: Does short-term summer precipitation increase faster?, 42, 1165–1172, https://doi.org/10.1002/2014GL062588, 2015.

Ban, N., Rajczak, J., Schmidli, J., and Schär, C.: Analysis of Alpine precipitation extremes using generalized extreme value theory in convection-resolving climate simulations, 55, 61–75, https://doi.org/10.1007/s00382-018-4339-4, 2020.

Berg, P., Moseley, C., and Haerter, J. O.: Strong increase in convective precipitation in response to higher temperatures, 6, 181–185, https://doi.org/10.1038/ngeo1731, 2013.

Berg, P., Christensen, O. B., Klehmet, K., Lenderink, G., Olsson, J., Teichmann, C., and Yang, W.: Precipitation extremes in a EURO-CORDEX 0.11° ensemble at hourly resolution, https://doi.org/10.5194/nhess-2018-362, 2018.

Berg, P., Christensen, O. B., Klehmet, K., Lenderink, G., Olsson, J., Teichmann, C., and Yang, W.: Summertime precipitation extremes in a EURO-CORDEX 0.11° ensemble at an hourly resolution, 19, 957–971, https://doi.org/10.5194/nhess-19-957-2019, 2019.

Berthou, S., Kendon, E. J., Rowell, D. P., Roberts, M. J., Tucker, S., and Stratton, R. A.: Larger Future Intensification of Rainfall in the West African Sahel in a Convection-Permitting Model, 46, 13 299–13 307, https://doi.org/10.1029/2019GL083544, 2019.

Blanchet, J., Ceresetti, D., Molinié, G., and Creutin, J.-D.: A regional GEV scale-invariant framework for Intensity–Duration–Frequency analysis, 540, 82–95, https://doi.org/10.1016/j.jhydrol.2016.06.007, 2016.

Blöschl, G. and Sivapalan, M.: Scale issues in hydrological modelling: A review, 9, 251–290, https://doi.org/10.1002/hyp.3360090305, 1995.

Bodian, A., Ndiaye, O., and Dacosta, H.: Evolution des caractéristiques des pluies journalières dans le bassin versant du fleuve Sénégal: Aavant et après rupture, 61, 905–913, https://doi.org/10.1080/02626667.2014.950584, 2016.

Burlando, P. and Rosso, R.: Scaling and multiscaling models of depth-duration-frequency curves for storm precipitation, 1996.

Cannon, A. J. and Innocenti, S.: Projected intensification of sub-daily and daily rainfall extremes in convection-permitting climate model simulations over North America: implications for future intensity–duration–frequency curves, 19, 421–440, https://doi.org/10.5194/nhess-19-421-2019, 2019.

Centre for Environmental Data Analysis (CEDA): CP4-Africa dataset, https://catalogue.ceda.ac.uk/uuid/a6114f2319b34a58964dfa5305652fc6/, 2018.

https://doi.org/10.5194/egusphere-2026-6628
Preprint. Discussion started: 30 October 2026
© Author(s) 2026. CC BY 4.0 License.

Chagnaud, G., Panthou, G., Vischel, T., Blanchet, J., and Lebel, T.: A unified statistical framework for detecting trends in multi-timescale precipitation extremes: application to non-stationary intensity-duration-frequency curves, 145, 839–860, https://doi.org/10.1007/s00704-021-03650-9, 2021.

Chagnaud, G., Panthou, G., Vischel, T., and Lebel, T.: Capturing and Attributing the Rainfall Regime Intensification in the West African Sahel with CMIP6 Models, 36, 1823–1843, https://doi.org/10.1175/JCLI-D-22-0412.1, 2023a.

Chagnaud, G., Panthou, G., Vischel, T., and Lebel, T.: Réviser les courbes intensité-durée-fréquence dans un contexte de nouvelle donne hydro-climatique : de la détection de tendances à l'application opérationnelle, 109, 2293 085, https://doi.org/10.1080/27678490.2023.2293085, 2023b.

Coles, S.: An introduction to statistical modeling of extreme values, Springer Series in Statistics, 2001.

Diedhiou, S., Rauch, M., Lahat Dieng, A., Bliefernicht, J., Sy, S., Sall, S. M., and Kunstmann, H.: Extreme rainfall in Dakar (Senegal): a case study for September 5, 2020, 6, 1439 404, https://doi.org/10.3389/frwa.2024.1439404, 2024.

Dosio, A., Jury, M. W., Almazroui, M., Ashfaq, M., Diallo, I., Engelbrecht, F. A., Klutse, N. A. B., Lennard, C., Pinto, I., Sylla, M. B., and Tamoffo, A. T.: Projected future daily characteristics of African precipitation based on global (CMIP5, CMIP6) and regional (CORDEX, CORDEX-CORE) climate models, 57, 3135–3158, https://doi.org/10.1007/s00382-021-05859-w, 2021.

Dunn, R. J. H., Alexander, L. V., Donat, M. G., Zhang, X., Bador, M., Herold, N., Lippmann, T., Allan, R., Aguilar, E., Barry, A. A., Brunet, M., Caesar, J., Chagnaud, G., Cheng, V., Cinco, T., Durre, I., De Guzman, R., Htay, T. M., Wan Ibadullah, W. M., Bin Ibrahim, M. K. I., Khoshkam, M., Kruger, A., Kubota, H., Leng, T. W., Lim, G., Li-Sha, L., Marengo, J., Mbatha, S., McGree, S., Menne, M., De Los Milagros Skansi, M., Ngwenya, S., Nkrumah, F., Oonariya, C., Pabon-Caicedo, J. D., Panthou, G., Pham, C., Rahimzadeh, F., Ramos, A., Salgado, E., Salinger, J., Sané, Y., Sopaheluwakan, A., Srivastava, A., Sun, Y., Timbal, B., Trachow, N., Trewin, B., Van Der Schrier, G., Vazquez-Aguirre, J., Vasquez, R., Villarroel, C., Vincent, L., Vischel, T., Vose, R., and Bin Hj Yussof, M. N.: Development of an Updated Global Land In Situ-Based Data Set of Temperature and Precipitation Extremes: HadEX3, 125, e2019JD032 263, https://doi.org/10.1029/2019JD032263, 2020.

Fosser, G., Gaetani, M., Kendon, E. J., Adinolfi, M., Ban, N., Belušić, D., Caillaud, C., Careto, J. A. M., Coppola, E., Demory, M.-E., De Vries, H., Dobler, A., Feldmann, H., Goergen, K., Lenderink, G., Pichelli, E., Schär, C., Soares, P. M. M., Somot, S., and Tölle, M. H.: Convection-permitting climate models offer more certain extreme rainfall projections, 7, 51, https://doi.org/10.1038/s41612-024-00600-w, 2024.

François, B., Schlef, K., Wi, S., and Brown, C.: Design considerations for riverine floods in a changing climate – A review, 574, 557–573, https://doi.org/10.1016/j.jhydrol.2019.04.068, 2019.

Galle, S., Grippa, M., Peugeot, C., Moussa, I. B., Cappelaere, B., Demarty, J., Mougin, E., Panthou, G., Adjomayi, P., Agbossou, E., Ba, A., Boucher, M., Cohard, J.-M., Descloitres, M., Descroix, L., Diawara, M., Dossou, M., Favreau, G., Gangneron, F., Gosset, M., Hector, B., Hiernaux, P., Issoufou, B.-A., Kergoat, L., Lawin, E., Lebel, T., Legchenko, A., Abdou, M. M., Malam-Issa, O., Mamadou, O., Nazoumou, Y., Pellarin, T., Quantin, G., Sambou, B., Seghieri, J., Séguis, L., Vandervaere, J.-P., Vischel, T., Vouillamoz, J.-M., Zannou, A., Afouda, S., Alhassane, A., Arjounin, M., Barral, H., Biron, R., Cazenave, F., Chaffard, V., Chazarin, J.-P., Guyard, H., Koné, A., Mainassara, I., Mamane, A., Oi, M., Ouani, T., Soumaguel, N., Wubda, M., Ago, E., Alle, I., Allies, A., Arpin-Pont, F., Awessou, B., Cassé, C., Charvet, G., Dardel, C., Depeyre, A., Diallo, F., Do, T., Fatras, C., Frappart, F., Gal, L., Gascon, T., Gibon, F., Guiro, I., Ingatan, A., Kempf, J., Kotchoni, D., Lawson, F., Leauthaud, C., Louvet, S., Mason, E., Nguyen, C., Perrimond, B., Pierre, C., Richard, A., Robert, E., Román-Cascón, C., Velluet, C., and Wilcox, C.: AMMA-CATCH, a Critical Zone Observatory in West Africa Monitoring a Region in Transition, 17, 1–24, https://doi.org/10.2136/vzj2018.03.0062, 2018.

https://doi.org/10.5194/egusphere-2026-6628
Preprint. Discussion started: 30 October 2026
© Author(s) 2026. CC BY 4.0 License.

Guerreiro, S. B., Fowler, H. J., Barbero, R., Westra, S., Lenderink, G., Blenkinsop, S., Lewis, E., and Li, X.-F.: Detection of continental-scale intensification of hourly rainfall extremes, 8, 803–807, https://doi.org/10.1038/s41558-018-0245-3, 2018.

Gupta, V. K. and Waymire, E.: Multiscaling properties of spatial rainfall and river flow distributions, 95, 1999–2009, https://doi.org/10.1029/JD095iD03p01999, 1990.

Jones, C. D., Hughes, J. K., Bellouin, N., Hardiman, S. C., Jones, G. S., Knight, J., Liddicoat, S., O'Connor, F. M., Andres, R. J., Bell, C., Boo, K.-O., Bozzo, A., Butchart, N., Cadule, P., Corbin, K. D., Doutriaux-Boucher, M., Friedlingstein, P., Gornall, J., Gray, L., Halloran, P. R., Hurtt, G., Ingram, W. J., Lamarque, J.-F., Law, R. M., Meinshausen, M., Osprey, S., Palin, E. J., Parsons Chini, L., Raddatz, T., Sanderson, M. G., Sellar, A. A., Schurer, A., Valdes, P., Wood, N., Woodward, S., Yoshioka, M., and Zerroukat, M.: The HadGEM2-ES implementation of CMIP5 centennial simulations, 4, 543–570, https://doi.org/10.5194/gmd-4-543-2011, 2011.

Kendon, E. J., Roberts, N. M., Senior, C. A., and Roberts, M. J.: Realism of Rainfall in a Very High-Resolution Regional Climate Model, 25, 5791–5806, https://doi.org/10.1175/JCLI-D-11-00562.1, 2012.

Kendon, E. J., Roberts, N. M., Fowler, H. J., Roberts, M. J., Chan, S. C., and Senior, C. A.: Heavier summer downpours with climate change revealed by weather forecast resolution model, 4, 570–576, https://doi.org/10.1038/nclimate2258, 2014.

Koutsoyiannis, D., Kozonis, D., and Manetas, A.: A mathematical framework for studying rainfall intensity-duration-frequency relationships, 206, 118–135, https://doi.org/10.1016/S0022-1694(98)00097-3, 1998.

Lebel, T., Cappelaere, B., Galle, S., Hanan, N., Kergoat, L., Levis, S., Vieux, B., Descroix, L., Gosset, M., Mougin, E., Peugeot, C., and Seguis, L.: AMMA-CATCH studies in the Sahelian region of West-Africa: An overview, 375, 3–13, https://doi.org/10.1016/j.jhydrol.2009.03.020, 2009.

Lenderink, G. and Van Meijgaard, E.: Linking increases in hourly precipitation extremes to atmospheric temperature and moisture changes, 5, 025 208, https://doi.org/10.1088/1748-9326/5/2/025208, 2010.

Madsen, H., Rasmussen, P. F., and Rosbjerg, D.: Comparison of annual maximum series and partial duration series methods for modeling extreme hydrologic events: 1. At-site modeling, 33, 747–757, https://doi.org/10.1029/96WR03848, 1997.

Martel, J.-L., Brissette, F. P., Lucas-Picher, P., Troin, M., and Arsenault, R.: Climate Change and Rainfall Intensity–Duration–Frequency Curves: Overview of Science and Guidelines for Adaptation, 26, 03121 001, https://doi.org/10.1061/(ASCE)HE.1943-5584.0002122, 2021.

Mathon, V., Laurent, H., and Lebel, T.: Mesoscale Convective System Rainfall in the Sahel, 41, 1081–1092, https://doi.org/10.1175/1520-0450(2002)041<1081:MCSRIT>2.0.CO;2, 2002.

Menabde, M., Seed, A., and Pegram, G.: A simple scaling model for extreme rainfall, 35, 335–339, https://doi.org/10.1029/1998WR900012, 1999.

Michelangeli, P., Vrac, M., and Loukos, H.: Probabilistic downscaling approaches: Application to wind cumulative distribution functions, 36, 2009GL038 401, https://doi.org/10.1029/2009GL038401, 2009.

Miller, J., Taylor, C., Guichard, F., Peyrillé, P., Vischel, T., Fowe, T., Panthou, G., Visman, E., Bologo, M., Traore, K., Coulibaly, G., Chapelon, N., Beucher, F., Rowell, D. P., and Parker, D. J.: High-impact weather and urban flooding in the West African Sahel – A multidisciplinary case study of the 2009 event in Ouagadougou, 36, 100 462, https://doi.org/10.1016/j.wace.2022.100462, 2022.

Milly, P. C. D., Betancourt, J., Falkenmark, M., Hirsch, R. M., Kundzewicz, Z. W., Lettenmaier, D. P., and Stouffer, R. J.: Stationarity Is Dead: Whither Water Management?, 319, 573–574, https://doi.org/10.1126/science.1151915, 2008.

Monerie, P.-A., Sanchez-Gomez, E., Gaetani, M., Mohino, E., and Dong, B.: Future evolution of the Sahel precipitation zonal contrast in CESM1, 55, 2801–2821, https://doi.org/10.1007/s00382-020-05417-w, 2020.

https://doi.org/10.5194/egusphere-2026-6628
Preprint. Discussion started: 30 October 2026
© Author(s) 2026. CC BY 4.0 License.

Nguyen, T., Kravitz, B., O'Brien, T. A., Ficklin, D. L., Rasmussen, K. L., Kruczkiewicz, A., Huang, J., Li, T., and Lauer, A.: Future Intensity-Duration-Frequency Curves of Extreme Precipitation in the Midwest United States From Convection-Permitting Modeling, 130, e2024JD042 798, https://doi.org/10.1029/2024JD042798, 2025.

Panthou, G., Vischel, T., Lebel, T., Blanchet, J., Quantin, G., and Ali, A.: Extreme rainfall in West Africa: A regional modeling, 48, 2012WR012 052, https://doi.org/10.1029/2012WR012052, 2012.

Panthou, G., Vischel, T., and Lebel, T.: Recent trends in the regime of extreme rainfall in the Central Sahel, 34, 3998–4006, https://doi.org/10.1002/joc.3984, 2014a.

Panthou, G., Vischel, T., Lebel, T., Quantin, G., and Molinié, G.: Characterising the space–time structure of rainfall in the Sahel with a view to estimating IDAF curves, 18, 5093–5107, https://doi.org/10.5194/hess-18-5093-2014, 2014b.

Panthou, G., Lebel, T., Vischel, T., Quantin, G., Sane, Y., Ba, A., Ndiaye, O., Diongue-Niang, A., and Diopkane, M.: Rainfall intensification in tropical semi-arid regions: the Sahelian case, 13, 064 013, https://doi.org/10.1088/1748-9326/aac334, 2018.

Prein, A. F., Langhans, W., Fosser, G., Ferrone, A., Ban, N., Goergen, K., Keller, M., Tölle, M., Gutjahr, O., Feser, F., Brisson, E., Kollet, S., Schmidli, J., Van Lipzig, N. P. M., and Leung, R.: A review on regional convection-permitting climate modeling: Demonstrations, prospects, and challenges, 53, 323–361, https://doi.org/10.1002/2014RG000475, 2015.

Sane, Y., Panthou, G., Bodian, A., Vischel, T., Lebel, T., Dacosta, H., Quantin, G., Wilcox, C., Ndiaye, O., Diongue-Niang, A., and Diop Kane, M.: Intensity–duration–frequency (IDF) rainfall curves in Senegal, 18, 1849–1866, https://doi.org/10.5194/nhess-18-1849-2018, 2018.

Schlef, K. E., Kunkel, K. E., Brown, C., Demissie, Y., Lettenmaier, D. P., Wagner, A., Wigmosta, M. S., Karl, T. R., Easterling, D. R., Wang, K. J., François, B., and Yan, E.: Incorporating non-stationarity from climate change into rainfall frequency and intensity-duration-frequency (IDF) curves, 616, 128 757, https://doi.org/10.1016/j.jhydrol.2022.128757, 2023.

Senior, C. A., Finney, D., Owiti, Z., Rowell, D., Marsham, J., Lawrence, J., Berthou, S., Kendon, E., and Misiani, H.: Technical guidelines for using CP4-Africa simulation data, Tech. Rep. Future climate for Africa-2020-11, Future climate for Africa, 2020.

Senior, C. A., Marsham, J. H., Berthou, S., Burgin, L. E., Folwell, S. S., Kendon, E. J., Klein, C. M., Jones, R. G., Mittal, N., Rowell, D. P., Tomassini, L., Vischel, T., Becker, B., Birch, C. E., Crook, J., Dougill, A. J., Finney, D. L., Graham, R. J., Hart, N. C. G., Jack, C. D., Jackson, L. S., James, R., Koelle, B., Misiani, H., Mwalukanga, B., Parker, D. J., Stratton, R. A., Taylor, C. M., Tucker, S. O., Wainwright, C. M., Washington, R., and Willet, M. R.: Convection-Permitting Regional Climate Change Simulations for Understanding Future Climate and Informing Decision-Making in Africa, 102, E1206–E1223, https://doi.org/10.1175/BAMS-D-20-0020.1, 2021.

Sharma, A., Hettiarachchi, S., and Wasko, C.: Estimating design hydrologic extremes in a warming climate: alternatives, uncertainties and the way forward, 379, 20190 623, https://doi.org/10.1098/rsta.2019.0623, 2021.

Sow, M., Dixon, R. D., Diakhaté, M., Guichard, F., Couvreux, F., and Gaye, A. T.: Contribution From the Occurrence and Intensity of Wet Days to the West African Rainfall Variability in CMIP6 Models, 52, https://doi.org/10.1029/2024GL110022, 2025.

Stratton, R. A., Senior, C. A., Vosper, S. B., Folwell, S. S., Boutle, I. A., Earnshaw, P. D., Kendon, E., Lock, A. P., Malcolm, A., Manners, J., Morcrette, C. J., Short, C., Stirling, A. J., Taylor, C. M., Tucker, S., Webster, S., and Wilkinson, J. M.: A Pan-African Convection-Permitting Regional Climate Simulation with the Met Office Unified Model: CP4-Africa, 31, 3485–3508, https://doi.org/10.1175/JCLI-D-17-0503.1, 2018.

Taylor, C. M., Belušić, D., Guichard, F., Parker, D. J., Vischel, T., Bock, O., Harris, P. P., Janicot, S., Klein, C., and Panthou, G.: Frequency of extreme Sahelian storms tripled since 1982 in satellite observations, 544, 475–478, https://doi.org/10.1038/nature22069, 2017.

https://doi.org/10.5194/egusphere-2026-6628
Preprint. Discussion started: 30 October 2026
© Author(s) 2026. CC BY 4.0 License.

Trenberth, K. E., Dai, A., Rasmussen, R. M., and Parsons, D. B.: The Changing Character of Precipitation, 84, 1205–1218, https://doi.org/10.1175/BAMS-84-9-1205, 2003.

Van De Vyver, H.: On the estimation of continuous 24-h precipitation maxima, 29, 653–663, https://doi.org/10.1007/s00477-014-0912-5, 2015.

Van De Vyver, H.: A multiscaling-based intensity–duration–frequency model for extreme precipitation, 32, 1635–1647, https://doi.org/10.1002/hyp.11516, 2018.

Van De Vyver, H., Van Schaeybroeck, B., De Troch, R., De Cruz, L., Hamdi, R., Villanueva-Birriel, C., Marbaix, P., Van Ypersele, J.-P., Wouters, H., Vanden Broucke, S., Van Lipzig, N. P., Doutreloup, S., Wyard, C., Scholzen, C., Fettweis, X., Caluwaerts, S., and Termonia, P.: Evaluation framework for sub-daily rainfall extremes simulated by regional climate models, https://doi.org/10.1175/JAMC-D-21-0004.1, 2021.

Van De Vyver, H., Van Schaeybroeck, B., De Cruz, L., Hamdi, R., and Termonia, P.: Bias-Adjustment Methods for Future Subdaily Precipitation Extremes Consistent Across Durations, 10, e2022EA002 798, https://doi.org/10.1029/2022EA002798, 2023.

Westra, S., Alexander, L. V., and Zwiers, F. W.: Global Increasing Trends in Annual Maximum Daily Precipitation, 26, 3904–3918, https://doi.org/10.1175/JCLI-D-12-00502.1, 2013.

Westra, S., Fowler, H. J., Evans, J. P., Alexander, L. V., Berg, P., Johnson, F., Kendon, E. J., Lenderink, G., and Roberts, N. M.: Future changes to the intensity and frequency of short-duration extreme rainfall: FUTURE INTENSITY OF SUB-DAILY RAINFALL, 52, 522–555, https://doi.org/10.1002/2014RG000464, 2014.

Willems, P.: Impacts of Climate Change on Rainfall Extremes and Urban Drainage Systems, 11, https://doi.org/10.2166/9781780401263, 2012.

Zhao, W., Abhishek, and Kinouchi, T.: Uncertainty quantification in intensity-duration-frequency curves under climate change: Implications for flood-prone tropical cities, 270, 106 070, https://doi.org/10.1016/j.atmosres.2022.106070, 2022.